Mol Neurobiol
DOI 10.1007/s12035-013-8451-5

CXCL12-Mediated Murine Neural Progenitor Cell Movement Requires PI3Kβ Activation

Borja L. Holgado · Laura Martínez-Muñoz · Juan Antonio Sánchez-Alcañiz · Pilar Lucas · Vicente Pérez-García · Gema Pérez · José Miguel Rodríguez-Frade · Marta Nieto · Óscar Marín · Yolanda R. Carrasco · Ana C. Carrera · Manuel Álvarez-Dolado · Mario Mellado

Received: 17 October 2012 / Accepted: 25 March 2013

Abstract The migratory route of neural progenitor/precursor cells (NPC) has a central role in central nervous system development. Although the role of the chemokine CXCL12 in NPC migration has been described, the intracellular signaling cascade involved remains largely unclear. Here we studied the molecular mechanisms that promote murine NPC migration in response to CXCL12, in vitro and ex vivo. Migration was highly dependent on signaling by the CXCL12 receptor, CXCR4. Although the JAK/STAT pathway was activated following CXCL12 stimulation of NPC, JAK activity was not necessary for NPC migration in vitro. Whereas CXCL12 activated the PI3K catalytic subunits p110α and p110β in NPC, only p110β participated in CXCL12-mediated NPC migration. Ex vivo experiments using organotypic slice cultures showed that p110β blockade impaired NPC exit from the medial ganglionic eminence. In vivo experiments using in utero electroporation nonetheless showed that p110β is dispensable for radial migration of pyramidal neurons. We conclude that PI3K p110β is activated in NPC in response to CXCL12, and its activity is necessary for immature interneuron migration to the cerebral cortex.

Keywords CXCR4 · Cell migration · p110β · Neural precursor · Interneuron · JAK

Introduction

The central nervous system originates from a pool of neural progenitor/precursor cells (NPC) that proliferate in a niche that lines the ventricles of the developing brain [1]. These NPC are organized spatially in distinct domains with different neuronal specification. Neural progenitor cells differentiate into neuronal precursors and immature neurons that often migrate long distances to their destinations, where they mature and establish appropriate connections [2]. Migration is thus an essential and precisely regulated process for brain development and function [3]. Two types of migration have been identified in the forebrain, radial migration (mainly cortical pyramidal neurons and cerebellar granular neurons), in which cells migrate radially from the progenitor zone, and tangential migration (mainly cortical and olfactory bulb interneurons), in which cells migrate perpendicular to the direction of radial migration. Migration of interneuron precursors continues throughout adulthood, along a highly restricted route termed the rostral migratory stream, which extends from the lateral ventricles towards the olfactory bulb [4]. These diverse migratory pathways are

Electronic supplementary material The online version of this article (doi:10.1007/s12035-013-8451-5) contains supplementary material, which is available to authorized users.

B. L. Holgado · L. Martínez-Muñoz · P. Lucas · V. Pérez-García · G. Pérez · J. M. Rodríguez-Frade · Y. R. Carrasco · A. C. Carrera · M. Mellado (✉)
Department of Immunology and Oncology,
Centro Nacional de Biotecnología/CSIC,
Darwin 3, Cantoblanco, 28049 Madrid, Spain
e-mail: mmellado@cnb.csic.es

J. A. Sánchez-Alcañiz · Ó. Marín
Developmental Neurobiology, Instituto de Neurociencias/CSIC,
03550 Sant Joan d'Alacant, Spain

M. Nieto
Department of Cellular and Molecular Biology, Centro Nacional de Biotecnología/CSIC, 28049 Madrid, Spain

M. Álvarez-Dolado
Centro Andaluz de Biología Molecular y Medicina Regenerativa,
Instituto de Neurociencias/CSIC, 41092 Sevilla, Spain

Published online: 19 April 2013

defined by chemoattractant or chemorepellent gradients of various molecules in the extracellular space, including epidermal growth factor (EGF) [5], hepatic growth factor (HGF) [6], fibroblast growth factor (FGF) [7], chemokines [8], neuregulins [9], and semaphorins [10].

Chemokines and their receptors were originally identified in the immune system, where they direct cell migration and have central roles in leukocyte trafficking and immune responses. The constitutively expressed chemokine CXCL12 and its receptor, CXCR4, are crucial for patterning and function in the immune and nervous systems, as they guide the positioning of various cell types in specific microenvironments. Both CXCL12- and CXCR4-deficient mice die perinatally and show a similar phenotype, with defects in B lymphopoiesis, bone marrow myelopoiesis, development of the cardiac ventricular septum, and derailed cerebellar neuron migration [11–13]. The CXCL12/CXCR4 pair triggers NPC proliferation [14] and migration [15, 16] in vitro and in vivo. During development, CXCL12 expression directs migration of hippocampal dentate granule cells [17], Cajal-Retzius neurons [18], cerebellar granular neurons [8], and cortical interneurons [16, 19] to their correct locations in the brain. Before they settle in the developing cortical plate (CP), migrating interneurons in the cortex disperse tangentially through the marginal zone (MZ) and the subventricular zone (SVZ) [20]. CXCL12 or CXCR4 deficiency causes disorganization of this migratory pattern and premature CP entry [19]. In the adult SVZ, CXCL12, and CXCR4 promote proliferative NPC homing to endothelial cells; in addition, CXCL12 increases neuron precursor motility in the SVZ to aid migration towards the olfactory bulb [21]. CXCL12 has been also implicated in brain repair after injury. Chemoattractants secreted following focal cerebral ischemia guide NPC from the SVZ of the lateral ventricles to the damage area [22]; the NPC use the vasculature as a scaffold, which facilitates migration through the parenchyma [22]. CXCL12 is upregulated in the area neighboring the ischemia lesion, and attracts NPC specifically to the damage area from a xenograft [23].

Whereas chemokine signaling in immune cells has been studied in detail, the molecular mechanisms that govern CXCL12-mediated NPC migration are not completely understood. As G protein-coupled receptors (GPCR), the chemokine receptors initiate their signal transduction pathways by activation of a G protein [24]. In most cases, the G protein involved is sensitive to pertussis toxin (PTx) ($G_{i/o}$), although this specificity appears to be cell type dependent [25]. Chemokines thus promote changes in intracellular cAMP and Ca^{2+} levels [26], activate phospholipase C (PLC) [27], extracellular signal-regulated kinases (Erk-1/2) [28], and phosphatidylinositol 3-kinase (PI3K) [14, 29], whose substrate is Akt. Some reports also indicate that chemokines promote JANUS kinase (JAK) signaling pathway activation [30]. The PI3K, which phosphorylate the 3-hydroxyl group of the phosphatidylinositide inositol ring, are divided into three classes (I, II, and III). Class I PI3K is comprised of a regulatory and a catalytic subunit (p110) that has four isoforms (p110α, β, δ, and γ). All of them synthesize phosphatidylinositol-3,4,5-trisphosphate in cell membranes as a second messenger, which coordinates localization and function of many effector proteins that bind to these lipids through the pleckstrin homology domain [31]. PI3K have a central regulatory role in many cell processes including growth, survival, proliferation, and motility [31].

Here we analyzed CXCL12-triggered signaling pathways in neurosphere-derived NPC. Whereas we observed CXCL12-mediated JAK/STAT activation, NPC migration was JAK independent, at difference from immune system cells. We also detected CXCL12 activation of PI3K; using chemical inhibitors and shRNA expression, we found that CXCL12-induced migration was p110β dependent. The results indicate that, in addition to their known role in NPC survival, proliferation, and self-renewal [32, 33], the PI3K also regulate NPC movement in an isoform-specific manner.

Materials and Methods

Antibodies We used the following antibodies: anti-Erk-1, anti-Erk-2 (both rabbit), anti-phospho Erk-1/2 (mouse), anti-$G\alpha_i$ (rabbit), anti-STAT 5b (rabbit), and anti-p110β (rabbit) (all from Santa Cruz Biotechnologies); anti-β-actin (mouse), anti-β-tubulin (mouse), anti-β-tubulin isotype III (mouse), anti-mouse IgM-agarose (goat), and anti-mouse IgG-agarose (goat) (Sigma Aldrich); anti-Akt (rabbit), anti-phospho Akt (Thr 308, rabbit), and anti-JAK2 (rabbit) (Cell Signaling); anti-nestin (rabbit; Covance), anti-mouse CXCL12 (rabbit; eBioscience), anti-GFAP (mouse; Abcam), anti-mouse CXCR4 (biotinylated, rat), and anti-mouse IgG2b (biotinylated, rat; both from BD Pharmingen); and anti-CXCR4 (mouse[34]) and anti-SMC3 (rabbit; Chemicon International). As second antibodies, we used Alexa488-labeled goat anti-mouse IgG, Cy3-goat anti-rabbit IgG, Cy3-goat anti-mouse IgM (all from Molecular Probes), and horseradish peroxidase–goat anti-mouse and anti-rabbit Ig (Dako Cytomation). We also used phycoerythrin-avidin (Beckman Coulter).

Plasmids and Oligonucleotides For interference assays, NPC were nucleofected with pRS shRNA p110βor pRS shRNA scramble (both from OriGene). Nucleofection efficiency was controlled by electroporating a green fluorescent protein (GFP) pEGFP-N3 plasmid (BD Bioscience). NPC were nucleofected with siRNA for target sequences on JAK1 (5′-GAAAAUGAAUUGAGUCGAU-3′; 5′-GAAA UCACCCACAUUGUAA-3′, 5′-CGCA UGAGGUUCU ACUUUA-3′; 5′-GCACAGGGACAGUAUGAUU-3′) (ON-TARGETplus SMARTpool siRNA, mouse JAK1) or

siRNA control (ON-TARGETplus SMARTpool, nontargeting siRNA; both from Dharmacon).

Isolation of NPC and Neurosphere Culture Murine NPC were isolated at embryonic day (E)14.5 from C57BL/6, p110$\delta^{-/-}$ [35] and p110$\gamma^{-/-}$ embryos [36] and at E11.5 from JAK2$^{+/-}$ embryos [37]. Briefly, a suspension of dissociated NPC from the telencephalic vesicles were seeded at 5×10^4/cm^2 and grown as neurospheres in DMEM/F12 medium (Gibco) with N2 supplement (Gibco), 4 μg/mL heparin (Sigma), 20 ng/mL bFGF (Peprotech), and 20 ng/mL EGF (Peprotech) in uncoated Petri dishes (Nunc) (37 °C, 5 % CO_2) [38]. After 6 to 10 days in culture, primary neurospheres were used for experiments. For single-cell suspensions, neurospheres were dissociated with 0.02 % PBS-EDTA.

Cell Migration Assay CFSE-labeled neurosphere-derived NPC (1.5×10^5 cell, 0.1 mL) were placed in the upper well of a 24-well transmigration chamber (8 μm pore, Transwell, Costar) coated with fibronectin (20 μg/mL, 4 °C, overnight, Sigma). In the lower well, 0.6 mL migration medium (DMEM/F12, N2 supplement, 4 μg/mL heparin, 1 ng/mL bFGF, and 1 ng/mL EGF) were placed alone or with CXCL12 (50 nM, Peprotech). Cells were allowed to migrate (16 h, 37 °C). To analyze migration, non-migrated cells (upper surface of the filter) were eliminated with a cotton swab, followed by fixing the filter (4 % PFA, 10 min, room temperature (RT)). Images of migrated cells (adhered to the lower filter surface) were acquired using a confocal microscope (Zeiss Axiovert LSM 510-Meta) and fluorescence determined as migrating NPC, and quantified (ImageJ 4.3 software). Migration was calculated by dividing the area of migrated cells by that of total fluorescent cells (input) and expressed as percentage.

Where indicated, NPC chemotaxis was evaluated as above with the inhibitors LY294002 (10 μM, pan-PI3K), Src Inhibitor I (10 μM, pan-Src), JAK2 Inhibitor II (10 μM), AG490 (50 μM, pan-JAK), FAK Inhibitor II (10 μM), Syk Inhibitor IV (10 μM, all from Calbiochem), TGX-221 (30 μM, p110β) or PIK-75 (0.01 μM, p110α; both from Cayman Chemical), and PTx (0.1 μg/mL, $G\alpha_i$; Sigma).

To study p110β in cell migration, NPC were co-nucleofected with pRS shRNA p110β or scramble and pEGFP-N3 (5:1 ratio). Cell migration was evaluated by following GFP$^+$ NPC migration by confocal microscopy. Migration of siRNA JAK1/scramble-nucleofected NPC was evaluated by CFSE staining as described above.

Time-Lapse Microscopy Fibronectin (20 μg/mL, 1 h, 37 °C)-coated cover slips (FCS2 chambers, Bioptechs) were incubated with CXCL12 (100 nM, 1 h, 37 °C). After washing, CFSE-labeled NPC (1.5×10^6 cells) were injected into the warmed (37 °C) chamber at time 0. Cells were allowed to settle (10 min), and confocal fluorescence and transmitted light images were acquired every 20 s for 90 min. All assays were performed in phenol red-free RPMI, with N_2 supplement, 4 μg/mL heparin, 1 ng/mL bFGF, and 1 ng/mL EGF. Images were acquired on a Zeiss Axiovert LSM 510-Meta inverted microscope (×20 objective) and cell tracking analyzed with Imaris 6.0 software (Bitplane). Graphs and statistical analyses were generated with Prism 5.0 software (GraphPad); the unpaired Student's *t* test was applied.

Cell Stimulation and Sample Preparation for Western Blot NPC (10^6 cell/mL) were cultured in depletion medium (DMEM/F12 with N2 supplement, 4 μg/mL heparin; 37 °C, 90 min) and stimulated with CXCL12 (50 nM). Cells were lysed with RIPA buffer (50 mM Tris–HCl pH 7.6, 0.25 % sodium deoxycholate, 1 % Igepal, 150 mM NaCl, 1 mM EDTA) with a protease/phosphatase inhibitor mixture (25 mM NaF, 1 mM PMSF, 10 μg/mL each leupeptin and aprotinin, 1 mM sodium orthovanadate; 30 min, 4 °C, continuous rocking), then centrifuged (15,000×*g*, 15 min, 4 °C).

For immunoprecipitation analysis, 10^7 cells were lysed with digitonin buffer (20 mM triethanolamine pH 8.0, 300 mM NaCl, 2 mM EDTA, 20 % glycerol, 1 % digitonin, plus protease/phophatase inhibitor mixture as above; 30 min, 4 °C, continuous rocking), then centrifuged (15,000×*g*, 15 min, 4 °C). Immunoprecipitation was performed essentially as described [39], using specific antibodies.

For nuclear extract preparation [40], CXCL12-treated NPC were washed with ice-cold PBS and resuspended in buffer A (0.1 % Triton X-100, 10 mM Hepes pH 7.9, 10 mM KCl, 1.5 mM $MgCl_2$, 0.34 M sucrose, 10 % glycerol, protease/phosphatase inhibitors as above; 10 min, 4 °C). Nuclei were centrifuged (3,500×*g*, 5 min, 4 °C) and lysed with modified RIPA buffer (20 mM Tris–HCl pH 8; 0.5 % sodium deoxycholate, 1 % Igepal, 0.1 % sodium dodecyl sulfate (SDS), 137 mM NaCl, 1 mM $MgCl_2$, 1 mM $CaCl_2$, 10 % glycerol, protease/phosphatase inhibitors as above; 30 min, 4 °C, continuous rocking) and centrifuged (15,000×*g*, 15 min, 4 °C).

For Western blot analysis, protein extracts were separated in SDS–polyacrylamide gel electrophoresis (SDS-PAGE), transferred to nitrocellulose membranes, and Western blot performed as described [39].

FACS Analysis For cell surface staining, neurospheres were dissociated with 0.02 % PBS-EDTA to preserve cell surface staining, filtered through a 40-μm cell strainer (Falcon) to obtain a single-cell suspension, plated in V-bottom 96-well plates (10^5 cells/well) and incubated with specific antibodies (0.5 μg/well, 30 min, 4 °C) in staining buffer (PBS, 0.1 %

fetal bovine serum, 1 % BSA, pH 7.0). Cells were washed twice and incubated with second antibody (15 min, 4 °C). Cell-bound fluorescence was determined in a Cytomics FC500 cytometer at 488 nm equipped with Cytomics CXP software (Beckman Coulter).

Cell Cycle Analysis After drug treatment, cell viability was determined by propidium iodide staining using the Coulter DNA PREP Reagents kit (Beckman Coulter).

Nucleofection NPC (6×10^6 cells/well) were nucleofected (3 μg/cuvette) with pRS shRNA p110β, pRS shRNA scramble (both from OriGene), siRNA JAK1 Smart Pool, and siRNA scramble (both from Dharmacon) using the Mouse NSC Nucleofector kit (Amaxa Biosciences).

Immunofluorescence NPC (5×10^5 cells/well) were plated on poly-L-lysine (Sigma)-coated cover slips (50 μg/mL, 1 h, 37 °C) and cultured (1 h, 37 °C). Cells were fixed (PBS, 4 % paraformaldehyde; 10 min, RT), washed with PBS with 150 mM NaCl, and permeabilized (PBS, 0.2 % Triton X-100, 150 mM NaCl, 10 min, RT). Cells were treated with blocking buffer (PBS with 1 % BSA, 0.1 % goat serum, 0.05 % Tween-20, 50 mM NaCl; 20 min, RT) before incubation with primary and secondary antibodies (20 min, RT, in the dark for both). Cover slips were mounted on microscope slides using Aqua Poly/Mount (Polysciences), and fluorescence evaluated in a confocal microscope (Axiovert LSM 510-Meta).

Slice Experiments and In Vitro Focal Electroporation Organotypic slice cultures of the embryonic mouse telencephalon were prepared as described [41]. pCAGGS-based GFP expression vectors were pressure-injected focally into the medial ganglionic eminence (MGE) of coronal slice cultures and focally electroporated [9]. Vehicle solution (DMSO) or TGX-221 (60 μM) was added to the medium after electroporation, replaced after 16 h, and slices cultured for another 24 h. For immunohistochemistry, slices were resectioned to 60 μm and incubated with rabbit anti-GFP (1:2,000, 4 °C, overnight), followed by Alexa488-donkey anti-rabbit (1:500, 2 h, RT; both from Invitrogen). Slices were mounted in Mowiol-Dabco with bisbenzamide (1:1,000, Sigma) and quantified using PhotoShop CS4 software (Adobe). Briefly, a calibration grid of concentric circles in 250 μm increments was located over the electroporation site in the MGE (point 0), and migrated cells were counted in six areas (0–250, 250–500, 500–750, 750–1,000, 1,000–1,250, and >1,250 μm) within the quadrant that included the cerebral cortex. Values were expressed as a percentage of total cells in the entire quadrant.

In Utero Electroporation In utero electroporation was performed as described [42]. Briefly, pRS shRNA p110μ plasmid (2 μg/μL) was mixed with pCAG-GFP (1 μg/μL), and pRS shRNA scramble (2 μg/μL) was mixed with pDsRed1-N1 (1 μg/μL) and used as a negative control. pRS shRNA p110β/pCAG-GFP mixture were injected in right lateral ventricle of E15.5 mouse embryo followed by electroporation. pRS shRNA scramble/pDsRed1-N1 mixture were then injected in the lateral ventricle of the left hemisphere in the same embryo. At E18.5, brains were fixed (PBS–4 % paraformaldehyde, pH 7.4; 16 h, 4 °C), cryoprotected (PBS–30 % sucrose; 16 h, 4 °C), and then embedded in OCT. Brain sections (30 μm thick) were stained with Hoechst 33258 and mounted in Aqua Poly/Mount (Polysciences). Fluorescence was evaluated in a confocal microscope (Axiovert LSM 510-Meta) and quantified with ImageJ 1.43 (NIH). Briefly, the cortex was divided in six equal bins, starting at the VZ (bin 1) and finishing at the pial surface (bin 6). Fluorescence in each bin was quantified and expressed as a percentage of total area of fluorescence in the entire quantified area.

Q-PCR Briefly, total RNA was extracted from cells using the RNeasy Micro Kit (Qiagen) or TRI reagent (Sigma), cDNA was prepared using SuperScript First-Strand Synthesis System for RT-PCR (Invitrogen), followed by Q-PCR using Power SYBR Green PCR Master mix (Applied Biosystems). All reactions were performed in the 7900 Real-Time PCR System (Applied Biosystems) as follows: 1 cycle 95 °C (10 min), followed by 40 cycles of 95 °C, 15 s and 60 °C, 1 min. Each sample was assessed in triplicate, and 28S expression was used to normalize copy number. Primer pairs used were: 28S forward 5′-TGCCATGGTAATCC TGCTCA-3′, 28S reverse 5′-CCTCAGCCAAGCA CATACACC-3′; JAK1 forward 5′-TGAGCTTTGATCGGA TCCTT-3′, JAK1 reverse 5′-GCAGGGTCCCA GAATAGATATG-3′; JAK2 forward 5′-GAACCTACAGATA CGGAGTGTCC-3′, JAK2 reverse 5′-CAAAATCAT GCCGCCACT-3′; JAK3 forward 5′-CACAGTGCATGG CCTATGAT-3′, JAK3 reverse 5′-AGGTGTGGGG TCTGAGAGG-3′; p110α forward 5′-GCTGGATTCAGTT ACTCCCATAC-3′, p110α reverse 5′-CGGAGCTGTT CCTTGTCATT-3′; p110β forward 5′-TCAGCATATGG GTTCGTCTG-3′, p110β reverse 5′-GCTGGTCTTC GTTTCCTGAT-3′; p110γ forward 5′-CCAGACAGTGTT TTTGTAAGAGGA-3′, p110γ reverse 5′-TCCATGCCCT ATGCGACT-3′; p110δ forward 5′-CCCGCTGATGC CAAAGTA-3′, p110δ reverse 5′-TGTTGTGTTACTT CTCTGAGGTCTG-3′. *X*-fold induction was calculated and expressed as $2^{-\Delta\Delta Ct}$.

PI3K Assay Neurosphere-derived NPC were lysed (50 mM Hepes pH 7.5, 150 mM NaCl, 10 % glycerol, 1 % Triton X-100, protease/phosphatase inhibitors as above). Protein (500 μg) from cell lysates was immunoprecipitated with

p110β-specific antibody and in vitro PI3K activity was measured as described [43] in the presence of TGX-221 (0.5 and 0.1 μM; p110β-specific inhibitor) or JAK2 Inhibitor II (10, 0.5, and 0.01 μM).

Results

CXCL12 Promotes Neurosphere-Derived NPC Migration

To study the signaling pathways involved in NPC migration, we used neurosphere-derived NPC. We used specific antibodies to detect CXCR4 expression at the cell surface by flow cytometry and immunofluorescence (Fig. 1a). Time-lapse microscopy studies showed that the receptor was fully functional, as determined by its ability to trigger CXCL12-induced NPC motility on fibronectin-coated plates (Fig. 1b and Online Resource 1). In these experiments, CXCL12 increased average speed (1.645±0.058 vs 1.964±0.044 μm/min; $p<0.001$; Fig. 1c) and total track length (145.5±5.7 vs 170.9±4.2 μm; $p<0.01$; Fig. 1d). In contrast, basal NPC motility increased on laminin- compared to fibronectin-coated plates (Online Resource 2a, b), and was CXCL12 independent (Online Resource 2c, d). These results indicate that NPC express a functional CXCR4 and that their motility depends on the chemokine and the substrate used.

As CXCL12 increased NPC motility, we used a chemotactic assay to evaluate NPC migration toward a CXCL12 gradient, after establishing the optimal CXCL12 concentration for these experiments (50 nM; Online Resource 3a). As for immune cells, CXCL12-induced NPC movement is $G\alpha_i$ dependent, as it was blocked by PTx treatment (Fig. 1e). Co-immunoprecipitation and Western blot analyses with specific antibodies showed that $G\alpha_i$ associated rapidly to CXCR4 in CXCL12-activated NPC (Fig. 1f). Treatment of NPC with the CXCR4 inhibitor AMD3100 abrogated the CXCL12-induced response (Fig. 1g). These results confirmed that neurosphere-derived NPC expressed a functional, $G\alpha_i$-dependent CXCR4 receptor responsible for the CXCL12-mediated effects. None of the treatments altered the NPC cell cycle (Online Resource 3b, c).

CXCL12 Triggers Distinct Signaling Cascades in NPC

In immune cells, CXCL12-mediated effects are dependent on JAK [30], PI3K [44], mitogen-activated protein kinase (MAPK) [28] and Src [45] signaling pathways. We used specific chemical inhibitors to identify the signals involved in NPC migration. Transmigration assays were performed with JAK2 Inhibitor II (10 μM [46]), AG490 (50 μM, pan-JAK inhibitor), FAK Inhibitor II (10 μM), Syk Inhibitor IV (10 μM), LY294002 (10 μM, PI3K inhibitor), or Src Inhibitor I (10 μM). NPC treated with JAK2 Inhibitor II, AG490, or LY294002 showed reduced CXCL12-mediated migration, whereas we found no significant differences in cells treated with Src Inhibitor I, FAK, or Syk inhibitors (Fig. 2). None of the treatments altered the NPC cell cycle (Online Resource 3d, e) or cell surface CXCR4 expression (not shown). The results suggested that JAK and PI3K are implicated in CXCL12-induced NPC migration.

To test CXCL12-mediated NPC signaling, we activated cells with 50 nM CXCL12 at different times and analyzed extracts by Western blot using anti-phospho Erk-1/2 and anti-phospho (Thr308) Akt antibodies (mAb). CXCL12 promoted Erk-1/2 and Akt activation, with a maximum at 1-min post-CXCL12 addition (Fig. 3a, b). To control loading, membranes were reblotted with anti-Erk-1/2 and anti-Akt antibodies.

We next lysed CXCL12-activated NPC, immunoprecipitated extracts with anti-phospho Tyr antibodies and analyzed lysates in Western blot using anti-JAK2 antibody. CXCL12 promoted rapid, transient JAK2 activation, reaching a maximum at 5 min post-stimulation (Fig. 3c). Chemokine-mediated JAK activation is followed by STAT binding to the chemokine receptor, its activation and translocation to the nucleus [47]. Extracts of CXCL12-activated NPC were immunoprecipitated using anti-CXCR4 mAb and developed in Western blot with anti-STAT5b antibody. CXCL12 promoted rapid, transient STAT5b association to CXCR4 (Fig. 3d). Evaluation of CXCL12-activated NPC nuclear extracts showed CXCL12-mediated STAT5b translocation to the nucleus (Fig. 3e). These results confirmed JAK, PI3K, and MAPK involvement in CXCL12-mediated functions in NPC.

JAK Signaling Pathway Is Not Involved in CXCL12-Mediated NPC Migration

To confirm JAK2 involvement in CXCL12-mediated NPC chemotaxis, we tested JAK expression in NPC isolated from wild-type (Wt) and $JAK2^{-/-}$ embryos. JAK1 mRNA levels were similar in both cell types, and were comparable with JAK2 mRNA levels in Wt NPC; JAK3 mRNA was barely detectable in either NPC type (Fig. 4a). We determined the ability of $JAK2^{-/-}$ NPC to migrate towards CXCL12 gradients in an in vitro chemotaxis assay; $JAK2^{-/-}$ NPC migrated normally (Fig. 4b), in contrast to results using JAK2 Inhibitor II. To rule out JAK1-mediated compensatory mechanisms, we used JAK1-specific siRNA (Fig. 4c) to knock down JAK1 expression in $JAK2^{-/-}$ NPC (Fig. 4d) and observed normal migration in response to CXCL12 (Fig. 4e). Our data suggest that neither JAK2 nor JAK1 has a role in NPC migration, at difference from results in other cell types [48], and that other kinases targeted by JAK2 Inhibitor II might be implicated in CXCL12-triggered NPC migration.

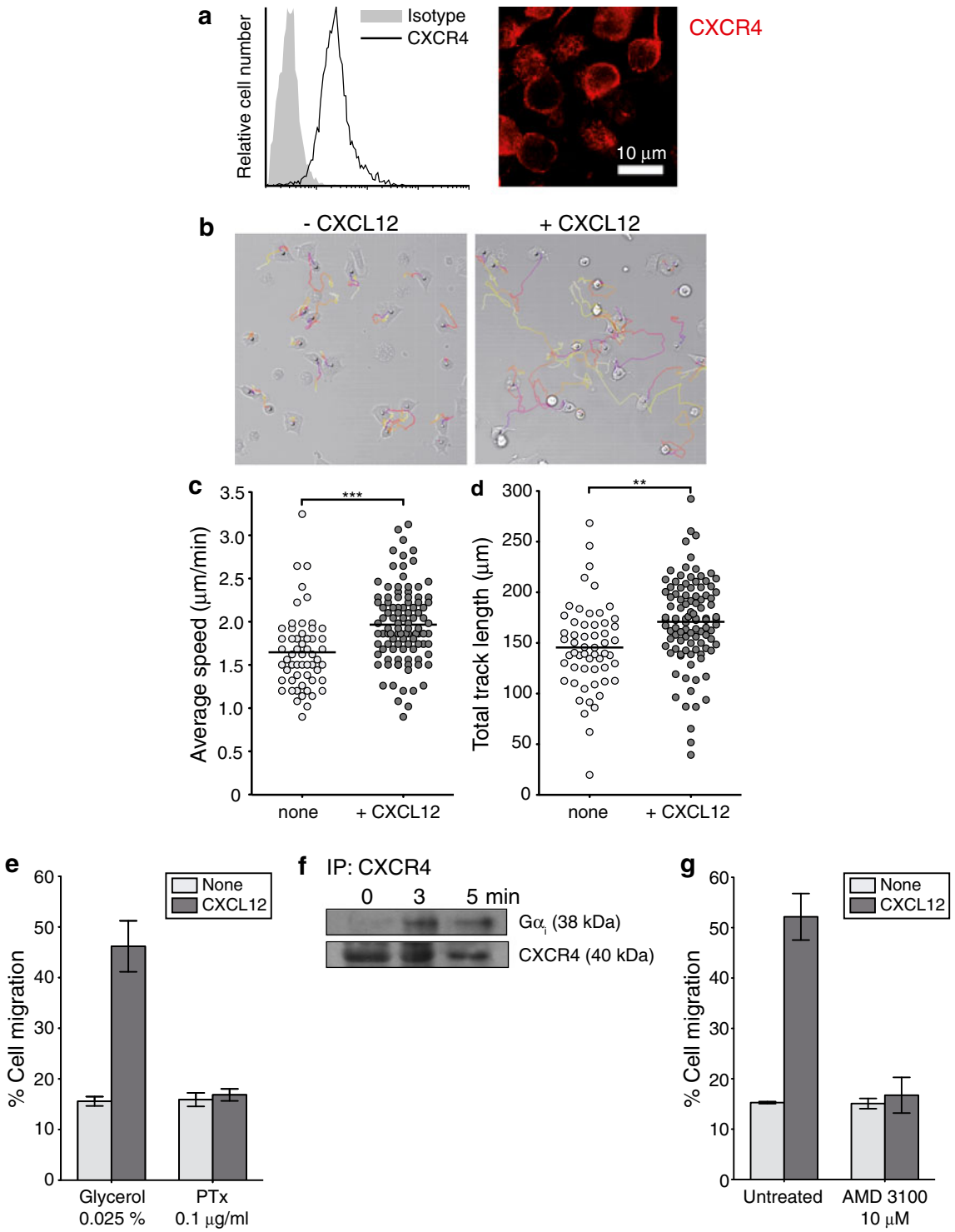

Fig. 1 CXCL12 promotes NPC migration **a** CXCR4 expression on the NPC surface was detected by flow cytometry analysis (*left*) and immunofluorescence (*right*) using specific antibodies. **b** Analysis of NPC motility by videomicroscopy; representative time-lapse images on fibronectin-coated surfaces with (*right*) or without (*left*) CXCL12. Each *dot* is a cell, and *lines* represent total track length. **c** Quantitation of the average speed from experiments in (**b**) (none, $n=56$ cells; CXCL12, $n=101$ cells). Student's t test; $^{***}P<0.001$. **d** Quantitation of total track length from experiments in (**b**) (none, $n=56$ cells; CXCL12, $n=101$ cells). $^{**}P<0.01$. **e** Glycerol- (0.025 %; control) or PTx-treated NPC were allowed to migrate in response to 50 nM CXCL12. Figure shows the percentage of migrated cells expressed as mean±SEM ($n=3$). **f** Lysates of CXCL12-activated NPC cells were immunoprecipitated with anti-CXCR4 mAb and the Western blot developed with anti-$G\alpha_i$ antibody. As protein loading control, the membrane was reprobed with anti-CXCR4 mAb. **g** Untreated or AMD3100-treated NPC were allowed to migrate in response to 50 nM CXCL12. The figure shows the percentage of migrated cells expressed as mean±SEM ($n=3$)

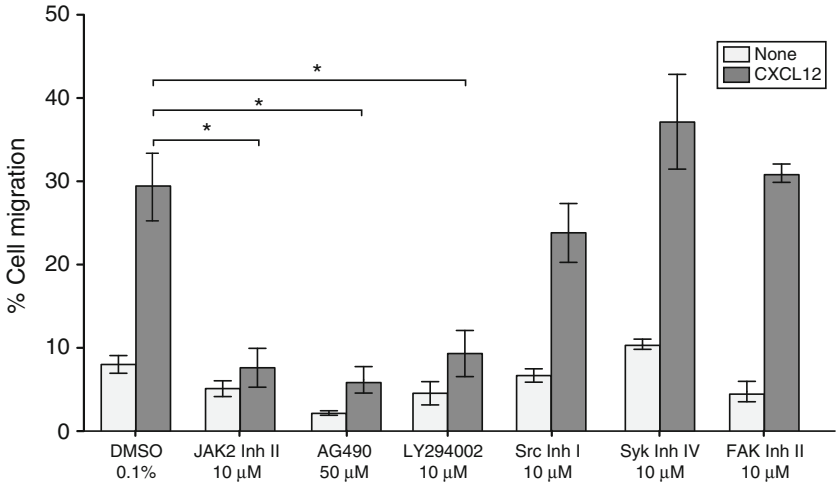

Fig. 2 CXCL12-mediated NPC migration depends on JAK and on PI3K activation CXCL12 (50 nM)-induced NPC migration was evaluated in the presence of JAK2 Inhibitor II (10 μM), LY294002 (10 μM), Src Inhibitor I (10 μM), AG490 (50 μM), or Syk Inhibitor IV (10 μM). As a control, cells were treated with 0.1 % DMSO. Data are expressed as mean±SEM (n=3). Student's t test; *P<0.05, *n.s.* not significant

p110β Is Necessary for CXCL12-Mediated NPC Migration

Although class I PI3K modulate cell migration, there is evidence that the isoform implicated is cell type and/or stimulus dependent [44]. Q-PCR analysis showed that NPC expressed high p110α and β and low p110γ and δ mRNA levels (Online Resource 4a), as confirmed in Western blot with specific antibodies (Online Resource 4b). To evaluate the role of p110γ and δ in migration, we isolated NPC from E14.5 p110γ- or δ-deficient mouse embryos, and found no defects in neurosphere formation (not shown) or in CXCL12-induced migration (Online Resource 4c, d). Given the low p110γ and δ levels and the unaltered migration of p110γ- or δ-deficient NPC, we focused on p110α and β. To test whether CXCL12 activated p110α or β in NPC, we analyzed Akt phosphorylation. Cells, untreated or treated with the p110α inhibitor PIK-75 (0.01 μM, 37 °C, 16 h) [49] or the p110β inhibitor TGX-221 (30 μM, 37 °C, 16 h) [50], were activated with 50 nM CXCL12 or 20 ng/mL EGF. Cell extracts were analyzed by Western blot using anti-p-Akt and anti-p-Erk-1/2 antibodies. Treatment with either inhibitor reduced CXCL12- and EGF-mediated Akt and Erk-1/2 phosphorylation (Fig. 5a). We tested inhibitor effect on NPC migration towards a CXCL12 gradient, and found that whereas p110α blockade had no effect, inhibition of p110β led to a marked reduction in cell migration (Fig. 5b). These data indicated that CXCL12 activates p110α and β in NPC, but only p110β is involved in migration.

To rule out a nonspecific effect of JAK2 Inhibitor II on p110β activity, we performed an in vitro kinase assay on p110β immunoprecipitates of NPC lysates in several concentrations of JAK2 Inhibitor II (10, 0.5, and 0.01 μM) and observed no alterations in p110β activity (Online Resource 5a). PI3Kβ activity was abrogated in the presence of TGX-221 (control) (Online Resource 5a). In Western blot, we found that JAK2 Inhibitor II treatment of NPC did not affect CXCL12-, EGF-, or LPA-mediated AKT phosphorylation (Online Resource 5b). Finally, TGX-221 treatment reduced CXCL12-mediated migration of JAK1/JAK2 double-deficient cells in in vitro chemotactic assays (Online Resource 5c). These results reinforce the idea that in NPC, CXCL12-mediated JAK and PI3K activation are independent signaling events.

To confirm the specific involvement of p110β, we used shRNA techniques to knock down p110β (Fig. 5c) in NPC before testing migration towards CXCL12. Control cells migrated normally, as predicted, whereas migration of p110β-deficient cells was reduced by >50 % (Fig. 5d). Moreover, control and p110β-silenced cells showed no alteration in surface CXCR4 levels, as indicated by flow cytometry analysis using specific antibody (Fig. 5e) or in p110α mRNA expression levels, as shown by Q-PCR analysis (Fig. 5c). Nucleofection efficiency was controlled by following GFP expression by FACS (Online Resource 4e). The results indicate that whereas CXCL12 activated both p110α and β only the latter modulated NPC migration in vitro.

p110β Modulates Interneuron But Not Pyramidal Cell Migration

To confirm the effect of p110β on NPC migration and validate our results in an ex vivo system, we used organotypic culture of mouse embryonic brain slices. In these assays, newborn GABAergic interneurons from the MGE migrate tangentially through the subpallium and reach the cortex, as occurs in vivo [41]. To label putative interneurons, we used focal electroporation of a GFP-encoding plasmid in the MGE of E13.5 telencephalic slices. Immediately after electroporation, slices were treated with TGX-221 (60 μM, 36 h, 37 °C) and cell localization was analyzed by fluorescence microscopy (Fig. 6a). TGX-221-treated cells were confined mainly to the MGE, with very limited tangential migration, whereas most untreated control interneurons migrated to the cortical area (Fig. 6b). Control cells

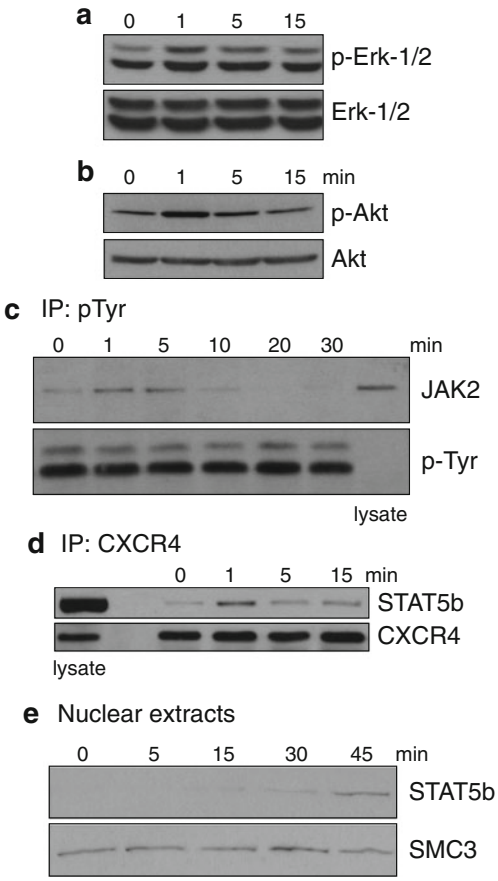

Fig. 3 CXCL12 triggers distinct signaling cascades in NPC. **a** Lysates of CXCL12-activated NPC cells were analyzed by Western blot and developed with anti-p-Erk-1/2 antibodies. As protein loading control, the membrane was reprobed with anti-Erk-1/2 mAb. **b** Cells as in (**a**) were evaluated by Western blot using anti-p-Akt antibody. As control, the membrane was reprobed with anti-Akt Ab. **c** Cells as in (**a**) were immunoprecipitated by p-Tyr mAb and then evaluated by Western blot using anti-p-JAK2 Ab. As control, the membrane was reprobed with anti-p-Tyr mAb. **d** Lysates of CXCL12-activated NPC cells were immunoprecipitated with anti-CXCR4 mAb and Western blot developed with anti-STAT5b Ab. As protein loading control, the membrane was reprobed with anti-CXCR4 mAb. **e** Nuclear extracts from CXCL12-activated NPC were lysed and evaluated by Western blot using anti-STAT5b Ab. As control, the membrane was reprobed with anti-SMC3 Ab

showed the migrating neuron morphology, with the leading neurite towards the cortex (Fig. 6c). Migrated cells were counted in six areas, at 0–250, 250–500, 500–750, 750–1,000, 1,000–1,250, and >1,250 μm, from the electroporation site at the MGE (Fig. 6d). More than 55.4±5.7 % of TGX-221 treated and only 22.7±3.2 % of control interneurons migrated less than 250 μm; approximately 3.5±1.2 % of TGX-221-treated and 12.4±1.9 % of control interneurons reached the 1,250 μm, and none of the treated cells exceeded this limit (Fig. 6e). The results confirmed the in vitro data and demonstrate an ex vivo effect of p110β on NPC migration.

To determine whether p110β-dependent NPC migration was restricted to immature interneurons, we used in utero electroporation to knock down p110β at the dorsal VZ-SVZ, and evaluated radial migration of pyramidal neurons from the neurogenic region towards the upper layers of the cortex. At E18.5, both DsRed/shRNA control and GFP/shRNA p110β-electroporated cells (bins 1–2) generated immature pyramidal neurons that migrated radially (bins 3, 4, 5, and 6) towards the pial surface with similar distributions (Fig. 7a and b, respectively). During this migratory process, DsRed/shRNA control and GFP/shRNA p110β cells showed the characteristic bipolar morphology of migrating pyramidal cells, with one leading neurite oriented towards the pial surface (Fig. 7c and d, respectively). Quantification of this experiment showed no significant differences between DsRed/shRNA control and GFP/shRNA p110β cells (Fig. 7e). These data showed that p110βis not necessary for pyramidal neuron migration, suggesting that the p110β role in migration is cell type and/or chemoattractant dependent.

Discussion

Cell movement is a key process in nervous system development [20], in adult neurogenesis [4, 51] and for the response to brain injury [22]. CXCL12 is one of the most studied chemoattractants for NPC, with important functions in embryogenesis [20] and during neuroblast migration in the SVZ of the lateral ventricles in adult brain [21]. Its expression is upregulated following brain injury and it guides NPC migration towards the site of insult [23]. We observed that embryonic NPC express CXCR4 and respond to CXCL12 in vitro. Videomicroscopy analyses of NPC motility showed that CXCL12 increased average speed and total track length on fibronectin-coated plates; these results concur with data for precursor cells from the medial ganglionic eminence [52], although our NPC moved more rapidly. Although we cannot rule out other possibilities, this difference in motility might be related to the experimental system used, to intrinsic cell differences, or to the substrate. Our assay used a two- rather than a three-dimensional system [52], which could affect average speed. We also detected a marked increase in basal NPC migration when laminin was used as substrate; in these conditions, cell movement appeared to be CXCL12 independent.

CXCL12-mediated NPC migration was blocked by AMD3100, a CXCR4-specific inhibitor, and by PTx. We also detected $G\alpha_i$ association to CXCR4 after CXCL12 stimulation, which confirmed that CXCR4 signaling is essential in CXCL12-induced NPC migration [15, 53]. CXCL12 also binds CXCR7 [54], another receptor implicated indirectly in NPC migration, which modulates

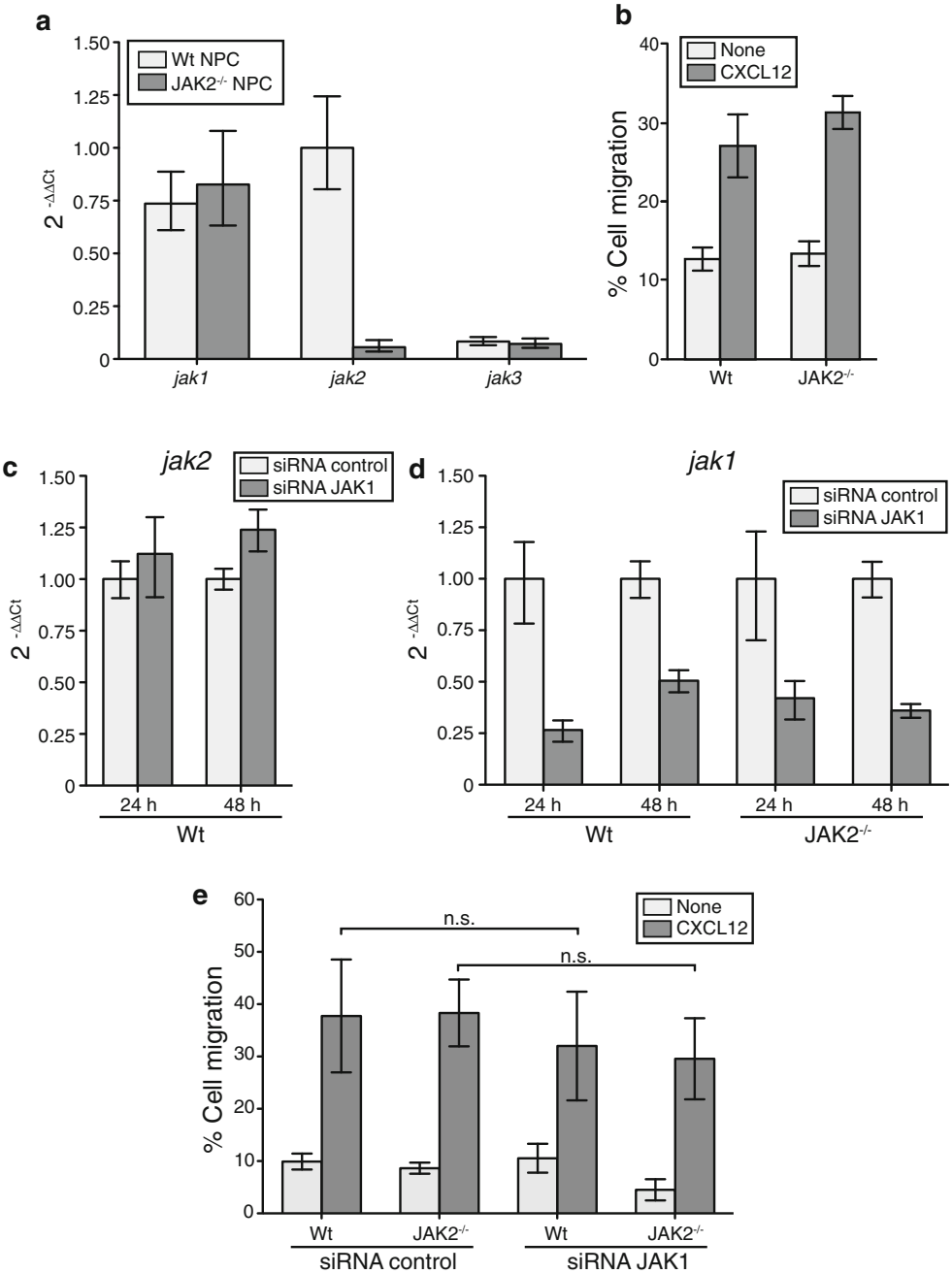

Fig. 4 Role of JAK/STAT pathway in CXCL12-mediated NPC migration. **a** Q-PCR analysis of JAK mRNA expression in Wt and JAK2$^{-/-}$ mouse NPC, using JAK2 mRNA levels in Wt NPC as reference. Data are expressed as mean±SEM (n=3). **b** NPC from Wt and JAK2$^{-/-}$ mice were allowed to migrate in response to 50 nM CXCL12. Figure shows the percentage of migrated cells expressed as mean±SEM (n=3). **c** JAK2 mRNA expression analyzed by Q-PCR in Wt and siRNA JAK1-nucleofected NPC. **d** Q-PCR analysis of JAK1 mRNA expression in Wt and JAK2$^{-/-}$ NPC nucleofected with siRNA for JAK1. **e** Wt and JAK2$^{-/-}$ mouse NPC were nucleofected with control or JAK1 siRNA; after 24 h, cells were allowed to migrate in response to 50 nM CXCL12. Figure shows the percentage of migrated cells expressed as mean±SEM (n=3). *n.s.* not significant

CXCL12 levels in vivo, preventing CXCR4 internalization [53].

We observed that NPC responded to CXCL12 by activating the JAK, PI3K, and Erk-1/2 pathways, all signaling events associated to CXCR4 in immune system cells [28, 34, 54, 55], and that CXCL12 promoted JAK2 activation and STAT5b association to CXCR4. JAK/STAT pathway activation by chemokines is reported for CCR2 [39], CCR7 [48], CCR5 [56], and CXCR4 [34]. The CXCR4 data are debated; some authors suggest that JAK2 or JAK3 deficiency does not alter CXCL12 responses in immune cells [57], whereas others implicate JAK in chemokine signaling, indicating that Tyr157 in the CXCR4 second intracellular loop is necessary for CXCL12-mediated STAT recruitment [58].

Our analyses indicated that CXCL12-induced NPC migration is blocked in cells treated with JAK2 Inhibitor II or with the pan-JAK inhibitor AG490, similar to results for T cells [30]. NPC from JAK2$^{-/-}$ mouse embryos and JAK2$^{-/-}$ NPC in which we knocked down JAK1 both migrated normally toward CXCL12 gradients. JAK proteins are therefore activated by CXCL12 in NPC, but do not participate in migration. CXCL12 might require the JAK/STAT pathway to trigger neural precursor differentiation, as shown

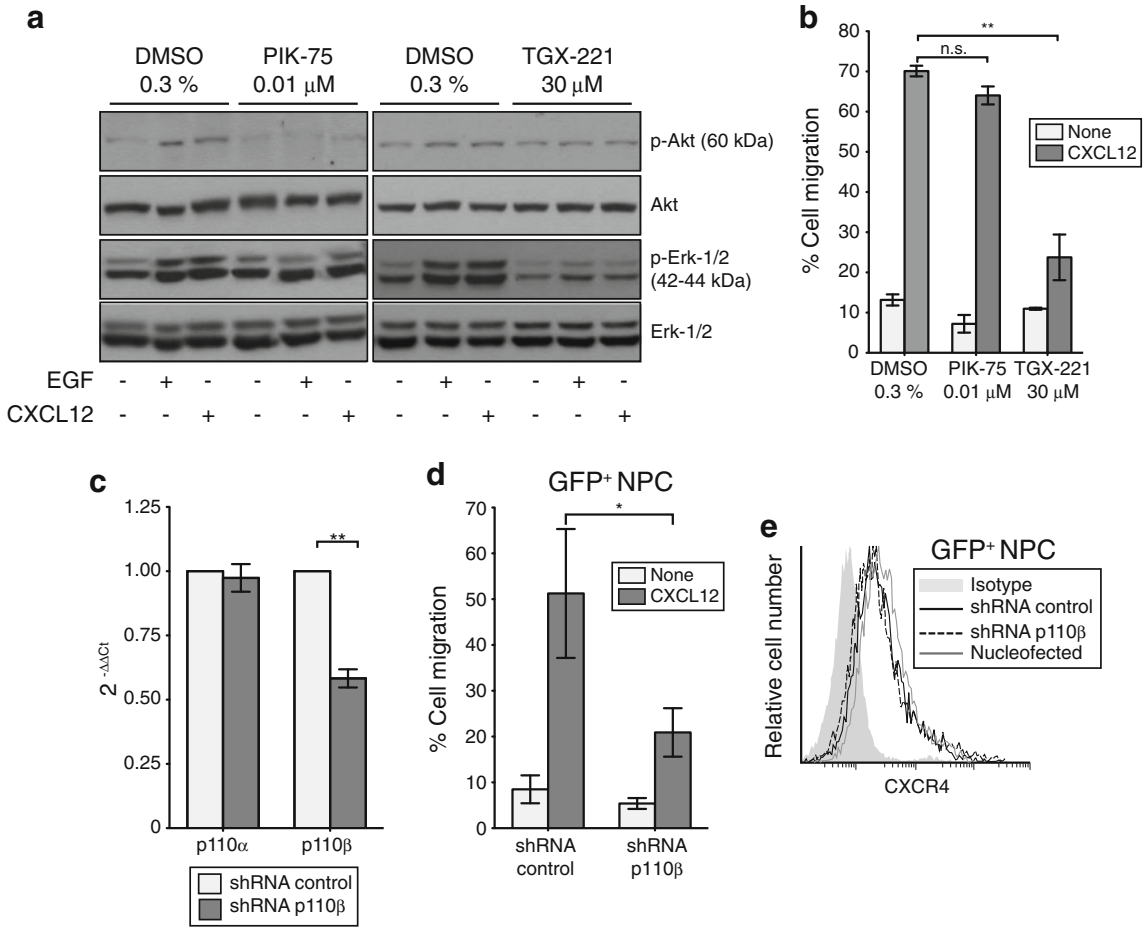

Fig. 5 p110β is necessary for CXCL12-mediated NPC migration. **a** NPC treated with PIK-75 (p110α inhibitor, 0.01 μM, 16 h) or TGX-221 (p110β inhibitor, 30 μM) were activated with CXCL12 (50 nM) or EGF (20 ng/mL) and lysed. As control, cells were treated with 0.3 % DMSO. Phosphorylation of Akt and Erk-1/2 was evaluated by Western blot using specific antibodies. Protein loading was controlled by reprobing the membrane with anti-Akt or -Erk-1/2 Ab. **b** 0.3 % DMSO (control), PIK-75 (0.01 μM)- and TGX-221 (30 μM)-treated NPC were allowed to migrate in response to 50 nM CXCL12. Data show mean±SEM (n=3). Student's t test; $^{**}P<0.01$. **c** p110α and p110β mRNA expression was analyzed by Q-PCR in shRNA control and shRNA p110β-nucleofected NPC. Data show mean±SEM (n=3). $^{**}P<0.01$. **d** shRNA control- or shRNA p110β-nucleofected NPC were allowed to migrate towards CXCL12 (50 nM). In these assays, NPC were co-nucleofected with pEGFP (5:1 shRNA/GFP ratio). Only GFP^+ NPC migration was quantified. Data show mean±SEM (n=6). $^{*}P<0.05$. **e** CXCR4 expression in shRNA control- or shRNA p110β-nucleofected NPC was determined by flow cytometry analysis of the GFP^+ population

for IL-6 cytokine family-mediated NPC differentiation [59]. The effect of the JAK inhibitors must thus be due to a non-specific effect on other kinases involved in cytoskeletal rearrangement. We nonetheless observed that cells treated with FAK or Syk inhibitors showed normal CXCL12-induced migration. Although FAK is implicated in adhesion formation and disassembly during migration of several cell types [60], its role in neuron migration is debated [61, 62]. Our data are compatible with a recent report showing that FAK is dispensable for glial-independent migration of interneurons [63].

PI3K is central to immune cell migration, although the isoform involved depends on the cell type studied; for example, neutrophils and T cells isolated from $p110\gamma^{-/-}$ mice show migration defects, although monocytes do not [64], and p110δ is necessary for glioma cell migration and invasion [65]. PI3K activation in NPC is associated with proliferation and survival [14]. We found that PI3K also participates in CXCL12-induced migration, probably because it is needed for actin filament remodeling [44]. Similar data were derived from in vitro studies of NPC treated with pan-PI3K inhibitors and stimulated with EGF [66], FGF [67], brain-derived neurotrophic factor [66], and Nrg1 [68].

p110α and p110β are the two main PI3K isoforms in NPC, both of which were activated by EGF and CXCL12 stimulation. Pretreatment with the p110α inhibitor PIK-75 or the p110β inhibitor TGX-221 blocked Akt phosphorylation. Only TGX-221 markedly reduced CXCL12-induced NPC migration, however, indicating that the β isoform is responsible for NPC movement toward chemoattractant

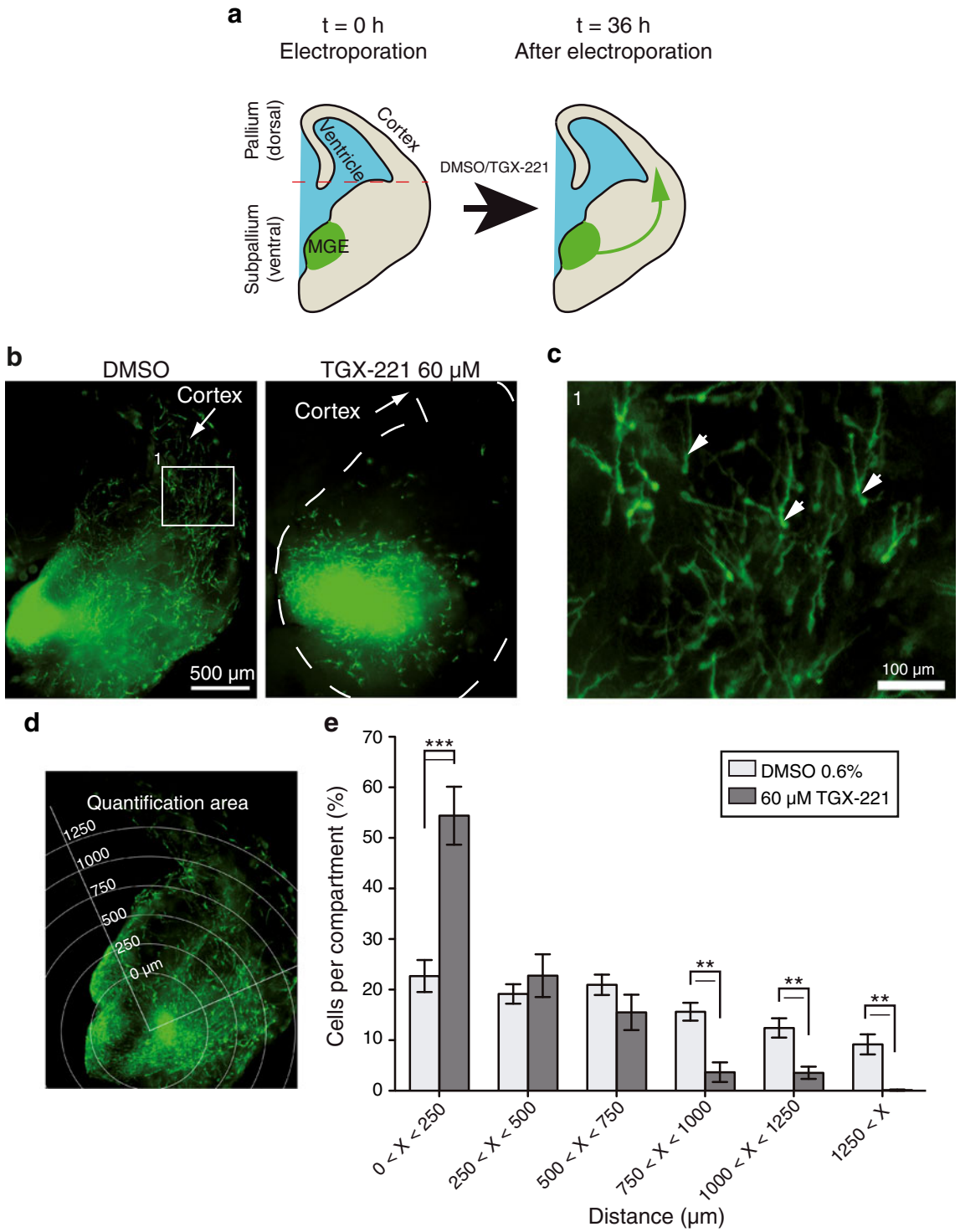

Fig. 6 p110β participates in ex vivo interneuron migration. **a** Scheme of organotypic assay. The medial ganglionic eminence (*MGE*) was electroporated with an EGFP-expressing plasmid to label migrating cells and brain sections, untreated or treated with 60 µM TGX-221 (36 h, 37 °C). Ex vivo interneuron migration (*green arrow*) to the cortex was then determined. **b** Representative images of brain sections treated with DMSO (0.6 %, control, *left*) or TGX-221 (60 µM, p110β inhibitor, *right*). **c** Zoom image of migrating interneurons (*box* in **b**). Cells are polarized (*arrowheads*) and extend the leading edge toward the cortex. **d** Calibrated grid used to quantitate cell migration distance. **e** Quantification of images as in (**b**). Values are mean±SEM of DMSO- ($n=7$) and TGX-221 ($n=8$)-treated brain slices in independent experiments. Student's t test; $^{**}P<0.01$, $^{***}P<0.001$

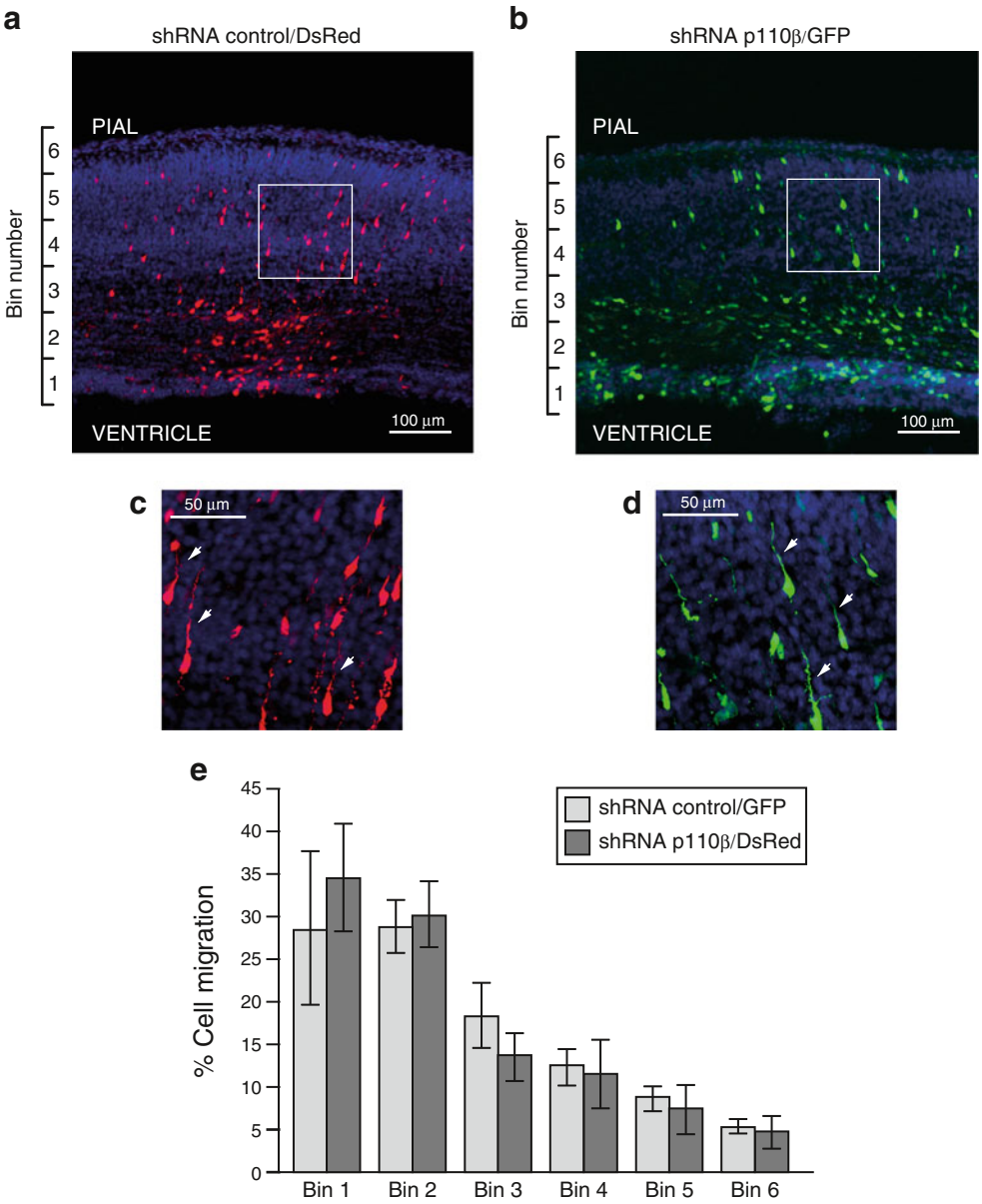

Fig. 7 p110β does not participate in in vivo pyramidal cell migration. Coronal sections of E18.5 cortex, electroporated in utero with **a** shRNA control/DsRed or **b** shRNA p110β/GFP. **c**, **d** Zoom image of migrating pyramidal neurons (*boxes* in **a** and **b**, respectively). Cell morphology is bipolar with the leading neurite (*arrowheads*) extended toward the pial surface. **e** Quantification of the distribution of DsRed- and GFP-expressing cells. *Numbers in ordinates* identify bins for quantification, from the ventricular zone (VZ, *bin 1*) to the marginal zone (MZ, *bin 6*). $n=4$ embryos. Student's t test; *ns* not significant

gradients. p110β is associated with S1P-induced endothelial cell migration via Rac1 activation [69], and evidence associates p110β to GPCR-triggered signaling pathways and p110α to growth factor signaling [55]. p110α activation is also linked to cell proliferation; indeed, constitutively active mutations of p110α are very common in cancer [31] and it is possible that CXCL12-mediated p110α activation is related to NPC proliferation. CXCL12-mediated NPC proliferation via PI3K has been reported [14]. p110β was also implicated in the control of DNA replication [70], although recent evidence assigns this effect to the p110β nuclear pool [71]. Studies in neuronal cell lines associate p85/p110 nuclear translocation with cell survival [72]. The mechanism that controls p110β intracellular location is not yet known; it is nonetheless plausible that whereas nuclear p110β regulates cell viability, the cytosolic pool participates in NPC migration.

We detected a clear reduction in Erk-1/2 activation when NPC were treated with the p110β inhibitor TGX-221, suggesting crosstalk between these two signaling pathways (Fig. 5a). Several reports indicate that cell migration is an Erk-1/2-dependent process [73–75], and connect PI3K and MAPK [76, 77]. Although further experiments are needed to confirm this observation, our preliminary data showed a marked reduction in CXCL12-mediated NPC migration after treatment with a specific Erk-1/2 pathway inhibitor (not shown).

In our experiments using NPC, p110β knockdown blocked CXCL12-induced migration. In the organotypic cultures, TGX-221 treatment abrogated MGE interneuron

precursor movement; whereas we found that pyramidal neuron migration was p110β independent. These data suggest a role for CXCL12 in NPC migration from the subpallium to the pallium, although evidence implicates Nrg1 as the main factor in this process. Consistent with these findings, an interneuron deficit is observed in the adult cerebral cortex of $Nrg1^{-/-}$ mice, and Ngr1 is detected throughout the subpallium during development [9]; this cortical interneuron deficit is not total in $Nrg1^{-/-}$ mice, however, suggesting the participation of other chemoattractants [9]. There are clear data indicating that $CXCL12^{-/-}$ mice do not show a reduction in cortical interneuron number, and that CXCL12 mRNA expression is restricted to the cortex during development, in accordance with its known role in promoting interneuron migration in the SVZ and MZ zones in the pallium [20]. The effects of chemokines are not always restricted to their expression sites, as chemokine binding to cell surface glycosaminoglycans generates chemotactic gradients [78], allowing long-distance effects. Moreover, recent analysis of mice deficient in either of the CXCL12 receptors (CXCR4 and CXCR7) showed an early delay in interneuron migration to the pallium, which is later compensated during development [15].

The role p110β in CXCL12-mediated NPC migration in vitro and the TGX-221-promoted inhibition of interneuron migration towards the cortex suggest that, in addition to Nrg1, CXCL12 could have a role in interneuron migration through the subpallium. We nonetheless cannot exclude the possibility that p110β participates in interneuron migration in response to other chemoattractants such as Nrg1. Our in utero electroporation assays showed no differences in the number or distribution of p110β-deficient pyramidal interneurons, concurring with involvement of other chemoattractants, such as reelin, in directing radial migration of pyramidal cells [2]. We thus consider that p110β-mediated migration is chemoattractant dependent, although we cannot rule out p110β triggering of migration in a cell-type-specific manner.

In conclusion, our data indicate that CXCL12-triggered NPC migration depends on class I PI3K activation; at difference from other cell systems, p110β participates in this process. p110β is essential for interneuron migration in a system that simulates in vivo conditions, suggesting its involvement in the migration of different NPC types in response to chemoattractants.

Acknowledgments We thank L. Gómez for animal handling, and C. Bastos and C. Mark for secretarial and editorial assistance, respectively. BLH received an FPI predoctoral fellowship (BES-2006-12965) from the Spanish Ministry of Science and Innovation. This work was supported in part by grants from the Spanish Ministry of Science and Innovation (SAF 2011-27370), the RETICS Program (RD08/0075/0010, RD12/0009/0009; RIER), the Madrid regional government (S2010/BMD-2350; RAPHYME), and the European Union (FP7-integrated project Masterswitch 223404).

References

1. Rakic P (2009) Evolution of the neocortex: a perspective from developmental biology. Nat Rev Neurosci 10(10):724–735
2. Ayala R, Shu T, Tsai LH (2007) Trekking across the brain: the journey of neuronal migration. Cell 128(1):29–43
3. Francis F, Meyer G, Fallet-Bianco C, Moreno S, Kappeler C, Socorro AC, Tuy FP, Beldjord C, Chelly J (2006) Human disorders of cortical development: from past to present. Eur J Neurosci 23(4):877–893
4. Ihrie RA, Alvarez-Buylla A (2011) Lake-front property: a unique germinal niche by the lateral ventricles of the adult brain. Neuron 70(4):674–686
5. Kornblum HI, Hussain RJ, Bronstein JM, Gall CM, Lee DC, Seroogy KB (1997) Prenatal ontogeny of the epidermal growth factor receptor and its ligand, transforming growth factor alpha, in the rat brain. J Comp Neurol 380(2):243–261
6. Powell EM, Mars WM, Levitt P (2001) Hepatocyte growth factor/scatter factor is a motogen for interneurons migrating from the ventral to dorsal telencephalon. Neuron 30(1):79–89
7. Guillemot F, Zimmer C (2011) From cradle to grave: the multiple roles of fibroblast growth factors in neural development. Neuron 71(4):574–588
8. Klein RS, Rubin JB, Gibson HD, DeHaan EN, Alvarez-Hernandez X, Segal RA, Luster AD (2001) SDF-1 alpha induces chemotaxis and enhances Sonic hedgehog-induced proliferation of cerebellar granule cells. Development 128(11):1971–1981
9. Flames N, Long JE, Garratt AN, Fischer TM, Gassmann M, Birchmeier C, Lai C, Rubenstein JL, Marin O (2004) Short- and long-range attraction of cortical GABAergic interneurons by neuregulin-1. Neuron 44(2):251–261
10. Marin O, Rubenstein JL (2001) A long, remarkable journey: tangential migration in the telencephalon. Nat Rev Neurosci 2(11):780–790
11. Ma Q, Jones D, Borghesani PR, Segal RA, Nagasawa T, Kishimoto T, Bronson RT, Springer TA (1998) Impaired B-lymphopoiesis, myelopoiesis, and derailed cerebellar neuron migration in CXCR4- and SDF-1-deficient mice. Proc Natl Acad Sci U S A 95(16):9448–9453
12. Nagasawa T, Hirota S, Tachibana K, Takakura N, Nishikawa S, Kitamura Y, Yoshida N, Kikutani H, Kishimoto T (1996) Defects of B-cell lymphopoiesis and bone-marrow myelopoiesis in mice lacking the CXC chemokine PBSF/SDF-1. Nature 382(6592):635–638
13. Zou YR, Kottmann AH, Kuroda M, Taniuchi I, Littman DR (1998) Function of the chemokine receptor CXCR4 in haematopoiesis and in cerebellar development. Nature 393(6685):595–599
14. Wu Y, Peng H, Cui M, Whitney NP, Huang Y, Zheng JC (2009) CXCL12 increases human neural progenitor cell proliferation through Akt-1/FOXO3a signaling pathway. J Neurochem 109(4):1157–1167
15. Wang Y, Li G, Stanco A, Long JE, Crawford D, Potter GB, Pleasure SJ, Behrens T, Rubenstein JL (2011) CXCR4 and CXCR7 have distinct functions in regulating interneuron migration. Neuron 69(1):61–76
16. Lopez-Bendito G, Sanchez-Alcaniz JA, Pla R, Borrell V, Pico E, Valdeolmillos M, Marin O (2008) Chemokine signaling controls intracortical migration and final distribution of GABAergic interneurons. J Neurosci 28(7):1613–1624
17. Bagri A, Gurney T, He X, Zou YR, Littman DR, Tessier-Lavigne M, Pleasure SJ (2002) The chemokine SDF1 regulates migration of dentate granule cells. Development 129(18):4249–4260
18. Paredes MF, Li G, Berger O, Baraban SC, Pleasure SJ (2006) Stromal-derived factor-1 (CXCL12) regulates laminar position of Cajal-Retzius cells in normal and dysplastic brains. J Neurosci 26(37):9404–9412

19. Stumm RK, Zhou C, Ara T, Lazarini F, Dubois-Dalcq M, Nagasawa T, Hollt V, Schulz S (2003) CXCR4 regulates interneuron migration in the developing neocortex. J Neurosci 23(12):5123–5130
20. Tiveron MC, Cremer H (2008) CXCL12/CXCR4 signalling in neuronal cell migration. Curr Opin Neurobiol 18(3):237–244
21. Kokovay E, Goderie S, Wang Y, Lotz S, Lin G, Sun Y, Roysam B, Shen Q, Temple S (2010) Adult SVZ lineage cells home to and leave the vascular niche via differential responses to SDF1/CXCR4 signaling. Cell Stem Cell 7(2):163–173
22. Zhang RL, Chopp M, Gregg SR, Toh Y, Roberts C, Letourneau Y, Buller B, Jia L, S PND, Zhang ZG (2009) Patterns and dynamics of subventricular zone neuroblast migration in the ischemic striatum of the adult mouse. J Cereb Blood Flow Metab 29(7):1240–1250
23. Imitola J, Raddassi K, Park KI, Mueller FJ, Nieto M, Teng YD, Frenkel D, Li J, Sidman RL, Walsh CA, Snyder EY, Khoury SJ (2004) Directed migration of neural stem cells to sites of CNS injury by the stromal cell-derived factor 1alpha/CXC chemokine receptor 4 pathway. Proc Natl Acad Sci U S A 101(52):18117–18122
24. Bokoch GM (1995) Chemoattractant signaling and leukocyte activation. Blood 86(5):1649–1660
25. Arai H, Charo IF (1996) Differential regulation of G-protein-mediated signaling by chemokine receptors. J Biol Chem 271(36):21814–21819
26. Ahmed MU, Hazeki K, Hazeki O, Katada T, Ui M (1995) Cyclic AMP-increasing agents interfere with chemoattractant-induced respiratory burst in neutrophils as a result of the inhibition of phosphatidylinositol 3-kinase rather than receptor-operated Ca^{2+} influx. J Biol Chem 270(40):23816–23822
27. Bacon KB, Flores-Romo L, Life PF, Taub DD, Premack BA, Arkinstall SJ, Wells TN, Schall TJ, Power CA (1995) IL-8-induced signal transduction in T lymphocytes involves receptor-mediated activation of phospholipases C and D. J Immunol 154(8):3654–3666
28. Schabath H, Runz S, Joumaa S, Altevogt P (2006) CD24 affects CXCR4 function in pre-B lymphocytes and breast carcinoma cells. J Cell Sci 119(Pt 2):314–325
29. Li S, Deng L, Gong L, Bian H, Dai Y, Wang Y (2010) Upregulation of CXCR4 favoring neural-like cells migration via AKT activation. Neurosci Res 67(4):293–299
30. Soriano SF, Serrano A, Hernanz-Falcon P, Martin de Ana A, Monterrubio M, Martinez C, Rodriguez-Frade JM, Mellado M (2003) Chemokines integrate JAK/STAT and G-protein pathways during chemotaxis and calcium flux responses. Eur J Immunol 33(5):1328–1333
31. Vanhaesebroeck B, Guillermet-Guibert J, Graupera M, Bilanges B (2010) The emerging mechanisms of isoform-specific PI3K signalling. Nat Rev Mol Cell Biol 11(5):329–341
32. Le Belle JE, Orozco NM, Paucar AA, Saxe JP, Mottahedeh J, Pyle AD, Wu H, Kornblum HI (2011) Proliferative neural stem cells have high endogenous ROS levels that regulate self-renewal and neurogenesis in a PI3K/Akt-dependant manner. Cell Stem Cell 8(1):59–71
33. Hu Q, Zhang L, Wen J, Wang S, Li M, Feng R, Yang X, Li L (2010) The EGF receptor-sox2-EGF receptor feedback loop positively regulates the self-renewal of neural precursor cells. Stem Cells 28(2):279–286
34. Vila-Coro AJ, Rodriguez-Frade JM, Martin De Ana A, Moreno-Ortiz MC, Martinez AC, Mellado M (1999) The chemokine SDF-1alpha triggers CXCR4 receptor dimerization and activates the JAK/STAT pathway. FASEB J 13(13):1699–1710
35. Okkenhaug K, Bilancio A, Farjot G, Priddle H, Sancho S, Peskett E, Pearce W, Meek SE, Salpekar A, Waterfield MD, Smith AJ, Vanhaesebroeck B (2002) Impaired B and T cell antigen receptor signaling in p110delta PI 3-kinase mutant mice. Science 297(5583):1031–1034
36. Sasaki T, Irie-Sasaki J, Jones RG, Oliveira-dos-Santos AJ, Stanford WL, Bolon B, Wakeham A, Itie A, Bouchard D, Kozieradzki I, Joza N, Mak TW, Ohashi PS, Suzuki A, Penninger JM (2000) Function of PI3Kgamma in thymocyte development, T cell activation, and neutrophil migration. Science 287(5455):1040–1046
37. Parganas E, Wang D, Stravopodis D, Topham DJ, Marine JC, Teglund S, Vanin EF, Bodner S, Colamonici OR, van Deursen JM, Grosveld G, Ihle JN (1998) Jak2 is essential for signaling through a variety of cytokine receptors. Cell 93(3):385–395
38. Rietze RL, Reynolds BA (2006) Neural stem cell isolation and characterization. Methods Enzymol 419:3–23
39. Mellado M, Rodriguez-Frade JM, Aragay A, del Real G, Martin AM, Vila-Coro AJ, Serrano A, Mayor F Jr, Martinez AC (1998) The chemokine monocyte chemotactic protein 1 triggers Janus kinase 2 activation and tyrosine phosphorylation of the CCR2B receptor. J Immunol 161(2):805–813
40. Méndez J, Stillman B (2000) Chromatin association of human origin recognition complex, cdc6, and minichromosome maintenance proteins during the cell cycle: assembly of prereplication complexes in late mitosis. Mol Cell Biol 20(22):8602–8612
41. Anderson SA, Eisenstat DD, Shi L, Rubenstein JL (1997) Interneuron migration from basal forebrain to neocortex: dependence on Dlx genes. Science 278(5337):474–476
42. Tabata H, Nakajima K (2001) Efficient in utero gene transfer system to the developing mouse brain using electroporation: visualization of neuronal migration in the developing cortex. Neuroscience 103(4):865–872
43. Jimenez C, Jones DR, Rodriguez-Viciana P, Gonzalez-Garcia A, Leonardo E, Wennstrom S, von Kobbe C, Toran JL, R-Borlado L, Calvo V, Copin SG, Albar JP, Gaspar ML, Diez E, Marcos MA, Downward J, Martinez AC, Merida I, Carrera AC (1998) Identification and characterization of a new oncogene derived from the regulatory subunit of phosphoinositide 3-kinase. EMBO J 17(3):743–753
44. Cain RJ, Ridley AJ (2009) Phosphoinositide 3-kinases in cell migration. Biol Cell 101(1):13–29
45. Montecucco F, Bianchi G, Gnerre P, Bertolotto M, Dallegri F, Ottonello L (2006) Induction of neutrophil chemotaxis by leptin. Ann N Y Acad Sci 1069(1):463–471
46. Sandberg EM, Ma X, He K, Frank SJ, Ostrov DA, Sayeski PP (2005) Identification of 1,2,3,4,5,6-hexabromocyclohexane as a small molecule inhibitor of jak2 tyrosine kinase autophosphorylation [correction of autophophorylation]. J Med Chem 48(7):2526–2533
47. Horvath CM, Wen Z, Darnell JE Jr (1995) A STAT protein domain that determines DNA sequence recognition suggests a novel DNA-binding domain. Genes Dev 9(8):984–994
48. Stein JV, Soriano SF, M'Rini C, Nombela-Arrieta C, de Buitrago GG, Rodriguez-Frade JM, Mellado M, Girard JP, Martinez AC (2003) CCR7-mediated physiological lymphocyte homing involves activation of a tyrosine kinase pathway. Blood 101(1):38–44
49. Knight ZA, Gonzalez B, Feldman ME, Zunder ER, Goldenberg DD, Williams O, Loewith R, Stokoe D, Balla A, Toth B, Balla T, Weiss WA, Williams RL, Shokat KM (2006) A pharmacological map of the PI3-K family defines a role for p110alpha in insulin signaling. Cell 125(4):733–747
50. Jackson SP, Schoenwaelder SM, Goncalves I, Nesbitt WS, Yap CL, Wright CE, Kenche V, Anderson KE, Dopheide SM, Yuan Y, Sturgeon SA, Prabaharan H, Thompson PE, Smith GD, Shepherd PR, Daniele N, Kulkarni S, Abbott B, Saylik D, Jones C, Lu L, Giuliano S, Hughan SC, Angus JA, Robertson AD, Salem HH (2005) PI 3-kinase p110[beta]: a new target for antithrombotic therapy. Nat Med 11(5):507–514

51. Ming GL, Song H (2011) Adult neurogenesis in the mammalian brain: significant answers and significant questions. Neuron 70(4):687–702
52. Lysko DE, Putt M, Golden JA (2011) SDF1 regulates leading process branching and speed of migrating interneurons. J Neurosci 31(5):1739–1745
53. Sanchez-Alcaniz JA, Haege S, Mueller W, Pla R, Mackay F, Schulz S, Lopez-Bendito G, Stumm R, Marin O (2011) Cxcr7 controls neuronal migration by regulating chemokine responsiveness. Neuron 69(1):77–90
54. Balabanian K, Lagane B, Infantino S, Chow KY, Harriague J, Moepps B, Arenzana-Seisdedos F, Thelen M, Bachelerie F (2005) The chemokine SDF-1/CXCL12 binds to and signals through the orphan receptor RDC1 in T lymphocytes. J Biol Chem 280(42):35760–35766
55. Guillermet-Guibert J, Bjorklof K, Salpekar A, Gonella C, Ramadani F, Bilancio A, Meek S, Smith AJ, Okkenhaug K, Vanhaesebroeck B (2008) The p110beta isoform of phosphoinositide 3-kinase signals downstream of G protein-coupled receptors and is functionally redundant with p110gamma. Proc Natl Acad Sci U S A 105(24):8292–8297
56. Wong M, Fish EN (1998) RANTES and MIP-1alpha activate stats in T cells. J Biol Chem 273(1):309–314
57. Moriguchi M, Hissong BD, Gadina M, Yamaoka K, Tiffany HL, Murphy PM, Candotti F, O'Shea JJ (2005) CXCL12 signaling is independent of Jak2 and Jak3. J Biol Chem 280(17):17408–17414
58. Ahr B, Denizot M, Robert-Hebmann V, Brelot A, Biard-Piechaczyk M (2005) Identification of the cytoplasmic domains of CXCR4 involved in Jak2 and STAT3 phosphorylation. J Biol Chem 280(8):6692–6700
59. Miller FD, Gauthier AS (2007) Timing is everything: making neurons versus glia in the developing cortex. Neuron 54(3):357–369
60. Mitra SK, Hanson DA, Schlaepfer DD (2005) Focal adhesion kinase: in command and control of cell motility. Nat Rev Mol Cell Biol 6(1):56–68
61. Beggs HE, Schahin-Reed D, Zang K, Goebbels S, Nave KA, Gorski J, Jones KR, Sretavan D, Reichardt LF (2003) FAK deficiency in cells contributing to the basal lamina results in cortical abnormalities resembling congenital muscular dystrophies. Neuron 40(3):501–514
62. Xie Z, Sanada K, Samuels BA, Shih H, Tsai LH (2003) Serine 732 phosphorylation of FAK by Cdk5 is important for microtubule organization, nuclear movement, and neuronal migration. Cell 114(4):469–482
63. Valiente M, Ciceri G, Rico B, Marin O (2011) Focal adhesion kinase modulates radial glia-dependent neuronal migration through connexin-26. J Neurosci 31(32):11678–11691
64. Ferguson GJ, Milne L, Kulkarni S, Sasaki T, Walker S, Andrews S, Crabbe T, Finan P, Jones G, Jackson S, Camps M, Rommel C, Wymann M, Hirsch E, Hawkins P, Stephens L (2007) PI(3)Kgamma has an important context-dependent role in neutrophil chemokinesis. Nat Cell Biol 9(1):86–91
65. Luk SK, Piekorz RP, Nurnberg B, Tony To SS (2012) The catalytic phosphoinositol 3-kinase isoform p110delta is required for glioma cell migration and invasion. Eur J Cancer 48(1):149–157
66. Zhang Q, Liu G, Wu Y, Sha H, Zhang P, Jia J (2011) BDNF promotes EGF-induced proliferation and migration of human fetal neural stem/progenitor cells via the PI3K/Akt pathway. Molecules 16(12):10146–10156
67. Glaser T, Brose C, Franceschini I, Hamann K, Smorodchenko A, Zipp F, Dubois-Dalcq M, Brustle O (2007) Neural cell adhesion molecule polysialylation enhances the sensitivity of embryonic stem cell-derived neural precursors to migration guidance cues. Stem Cells 25(12):3016–3025
68. Gambarotta G, Garzotto D, Destro E, Mautino B, Giampietro C, Cutrupi S, Dati C, Cattaneo E, Fasolo A, Perroteau I (2004) ErbB4 expression in neural progenitor cells (ST14A) is necessary to mediate neuregulin-1beta1-induced migration. J Biol Chem 279(47):48808–48816
69. Heller R, Chang Q, Ehrlich G, Hsieh SN, Schoenwaelder SM, Kuhlencordt PJ, Preissner KT, Hirsch E, Wetzker R (2008) Overlapping and distinct roles for PI3Kbeta and gamma isoforms in S1P-induced migration of human and mouse endothelial cells. Cardiovasc Res 80(1):96–105
70. Marques M, Kumar A, Poveda AM, Zuluaga S, Hernandez C, Jackson S, Pasero P, Carrera AC (2009) Specific function of phosphoinositide 3-kinase beta in the control of DNA replication. Proc Natl Acad Sci U S A 106(18):7525–7530
71. Kumar A, Redondo-Munoz J, Perez-Garcia V, Cortes I, Chagoyen M, Carrera AC (2011) Nuclear but not cytosolic phosphoinositide 3-kinase beta has an essential function in cell survival. Mol Cell Biol 31(10):2122–2133
72. Martelli AM, Faenza I, Billi AM, Manzoli L, Evangelisti C, Fala F, Cocco L (2006) Intranuclear 3′-phosphoinositide metabolism and Akt signaling: new mechanisms for tumorigenesis and protection against apoptosis? Cell Signal 18(8):1101–1107
73. Shi Y, Xia YY, Wang L, Liu R, Khoo KS, Feng ZW (2012) Neural cell adhesion molecule modulates mesenchymal stromal cell migration via activation of MAPK/ERK signaling. Exp Cell Res 318(17):2257–2267
74. Xu S, Menu E, De Becker A, Van Camp B, Vanderkerken K, Van Riet I (2012) Bone marrow-derived mesenchymal stromal cells are attracted by multiple myeloma cell-produced chemokine CCL25 and favor myeloma cell growth in vitro and in vivo. Stem Cells 30(2):266–279
75. Delgado-Martin C, Escribano C, Pablos JL, Riol-Blanco L, Rodriguez-Fernandez JL (2011) Chemokine CXCL12 uses CXCR4 and a signaling core formed by bifunctional Akt, extracellular signal-regulated kinase (ERK)1/2, and mammalian target of rapamycin complex 1 (mTORC1) proteins to control chemotaxis and survival simultaneously in mature dendritic cells. J Biol Chem 286(43):37222–37236
76. Bondeva T, Pirola L, Bulgarelli-Leva G, Rubio I, Wetzker R, Wymann MP (1998) Bifurcation of lipid and protein kinase signals of PI3Kgamma to the protein kinases PKB and MAPK. Science 282(5387):293–296
77. Lopez-Ilasaca M, Crespo P, Pellici PG, Gutkind JS, Wetzker R (1997) Linkage of G protein-coupled receptors to the MAPK signaling pathway through PI 3-kinase gamma. Science 275(5298):394–397
78. Janowski M (2009) Functional diversity of SDF-1 splicing variants. Cell adhesion & migration 3(3):243–249